Chemical Engineering Journal 422 (2021) 130150

Contents lists available at ScienceDirect

Chemical Engineering Journal

journal homepage: www.elsevier.com/locate/cej

Using an anion exchange membrane for effective hydroxide ion transport enables high power densities in microbial fuel cells

Ruggero Rossi, Bruce E. Logan *

Department of Civil and Environmental Engineering, The Pennsylvania State University, University Park, PA 16802, USA

ARTICLE INFO

Keywords:
Microbial fuel cell
Bioanode
pH imbalance
Anode acidification
Hydroxide ion transport
Power density

ABSTRACT

High current densities have been obtained by bioanodes in electrochemical cells, but this performance has not previously been translated into higher power densities in microbial fuel cells (MFCs). The most critical factor for boosting power generation in MFCs was proven here to be OH^- ion transfer from the cathode to the bioanode by comparing performance of an MFC with an anion exchange membrane (AEM), in a near zero-gap configuration and no bulk catholyte, to that obtained using a cation exchange membrane (CEM) or non-ion selective ultrafiltration membrane (UFM). In the AEM-MFC hydroxide ion transport primarily balanced charge transfer between the electrodes, enabling 8.8 ± 0.5 W m^{-2} (at 42 ± 1 A m^{-2}) which is highest power density ever achieved using this anolyte (acetate in a 50 mM phosphate buffer medium). The power density with the AEM was 3 × higher than that obtained using a CEM (3.1 ± 0.1 W m^{-2}) or UFM (2.4 ± 0.1 W m^{-2}) as these other two membranes allowed cations (sodium and magnesium) to be transported to the cathode for balancing charge. The lack of cation transport into the cathode using the AEM without a bulk catholyte also avoided salt precipitation in the cathode, and thus enabling more stable power production over time. The large differences in power obtained using the AEM, compared to the CEM or UFM conclusively demonstrate the critical role of OH^- ion transport in MFCs.

1. Introduction

Producing a high power density is a desired key feature of microbial fuel cells (MFCs), and accomplishing that requires electrodes capable of delivering high current densities with minimal internal resistance.[1–4] Bioanodes exploit the metabolism of exoelectrogenic microorganisms to generate electricity from the oxidation of organic substrate, and various materials and configurations have been used to increase current densities in different types of bioelectrochemical systems.[2,5–8] The highest current density produced was 390 A m^{-2} in a study by Chen et al. using six stacked layers of carbonized cardboard (70 A m^{-2} with one layer).[7] Other studies have reported up to 68 ± 3 A m^{-2} with a nanostructured reticulated vitreous carbon electrode,[6] and 129 A m^{-2} with an ice-templated titanium-based ceramic (ITTC) support.[5] Unfortunately, such high current densities have never been obtained in actual MFCs.[9] Assuming a cell operating voltage of 0.3 V and a current density of 70 A m^{-2} obtained by Chen at al.,[7] the maximum power would have been 21 W m^{-2}. However, when a single layer of the carbonized corrugated cardboard was tested in an actual MFC (treating human waste), the maximum current density was only 0.15 ± 0.05 A m^{-2} (with a power density on the order of 0.004 W m^{-2}) compared to 70 A m^{-2} obtained in the electrochemical reactor.[10] Bioanode performance in three electrode electrochemical reactors with stirring and cathode potentials adjusted to accommodate high current production by anodes avoid cathode mass transfer or kinetic limitations that will impact high current generation in an actual MFC.[11] Vigorous stirring with a highly buffered solution also minimizes mass-transfer limitations by providing better control of the local anode pH.

Maximizing power production of MFCs requires optimization of not only the anode performance, but also cathode performance, reactor architecture (sizes and distances between electrodes), and solution chemistry (buffer capacity and conductivity).[12,13] Although several strategies have been found to be effective in improving the MFC performance, many of these potential solutions are not practical, for example using chemical catholytes such as ferricyanide to boost the overall cell potential,[14] or adding salts or buffers to solutions media to increase the conductivity and reduce the solution resistance.[15] Another method is to use electrodes with different areas and then

* Corresponding author.
E-mail address: blogan@psu.edu (B.E. Logan).

https://doi.org/10.1016/j.cej.2021.130150
Received 23 March 2021; Received in revised form 24 April 2021; Accepted 27 April 2021
Available online 1 May 2021

normalize current and power by the smaller electrode. However, a more reasonable approach is to normalize to the cross-sectional area between the electrodes as that more accurately reflects overall system performance, or in H-cell MFC configurations to normalize based on electrode and tube areas and resistances.[16,17] Among these approaches increasing the buffer capacity of the media within limits that can be tolerated by the microorganisms is very effective for increasing the MFC performance.[18] When current generation in MFCs is limited by the development of differential pH between anode and cathode, increasing the buffer concentration will better enable pH near the electrodes to remain neutral.[11,15,19] Acetate oxidation at the anode can acidify the biofilm while the oxygen reduction reaction (ORR) at the cathode releases hydroxide ions, increasing the pH near the electrode, as shown by the two half-cell equations:[20]

$$CH_3COO^- + 4H_2O \rightleftharpoons HCO_3^- + H_2CO_3 + 8e^- + 8H^+ \quad (1)$$

$$O_2 + 4e^- + 2H_2O \rightleftharpoons 4OH^- \quad (2)$$

By using higher buffer concentrations the local pH can be maintained closer to neutral, which coupled with a lower solution resistance (higher salt content), allows higher current generation and larger cathode potentials.[18] However, increasing the buffer concentration is not practical for wastewater treatment due to cost concerns (and if phosphate is used, release of that nutrient into the environment) and increase in the solution salinity that can damage the bacteria on the anode.[18] Furthermore, all these methods have not resulted in large improvement of power output of MFCs, at least not enough to justify the additional efforts and material costs. For example, increasing the buffer capacity by 4 times in one study (from 50 mM to 200 mM) increased the maximum power by 80% (to 4.7 ± 0.2 W m^{-2})[21] but the current densities (<18 A m^{-2}) were still well below those achieved under more optimal conditions by others.[6,7] High performance can be obtained in MFCs with close electrode spacing as was recently reported by Rossi et al. using a zero-gap MFC with an AEM separating a flow-through bioanode and an air cathode.[22] The zero-gap configuration minimized the solution resistance, by diminishing the electrode spacing while ensuring electrical insulation. In that study it was assumed that the AEM was critical for improving performance by enabling OH^- ion transport, but that assumption was not directly tested, and thus it was not clear if the high maximum current (42 ± 1 A m^{-2}) and power density generated (5.7 ± 0.4 W m^{-2}) were due to the small electrode spacing, the use of the AEM, or the high flow rate in the anode chamber.

In this study, we demonstrate that efficient migration of hydroxide ions away from the cathode is the key factor for substantially increasing current and power production in MFC based on comparing performance of the AEM with two other types of separators, all in the zero-gap MFC configuration. While OH^- ion transport was assumed in previous studies to be the critical factor for improving power,[20,23] it is possible that the zero-gap design alone enabled high power production due to cation transport to balance charge, or by lowering internal resistance by using a more porous separator than an ion exchange membrane. Here, we prove that OH^- migration is an essential mechanism for achieving high power densities by showing that power densities are substantially reduced if the AEM is replaced by a cation exchange (CEM) or a porous ultrafiltration membrane (UFM) (Fig. 1). We hypothesized that using an AEM as a solid electrolyte pressed against a cathode, in the absence of bulk catholyte, would allow transport of primarily only OH^- ions generated by the ORR from cathode to the anolyte and anode (there would be minimal ion transfer of other ions due to concentration gradients). We reasoned that the only way to effectively test this hypothesis was by comparing performance using a CEM that would facilitate primarily cation transport, and a UFM that does not selectively transport ions based on charge. The lack of a bulk catholyte in this zero-gap design prevented transport of cations or anions other than OH^- ions that could lead to acidification of the local anode pH due to insufficient OH^- transfer to the anolyte. Such anolyte acidification has been routinely observed in many other studies using MFCs with catholytes and CEMs or AEMs.[24,25] Water needed for the ORR was provided here by a combination of water diffusion through the membrane anolyte and use of a humidified gas, thus eliminating the need for a bulk liquid catholyte. The selective transport of the OH^- directly next the anode further helps to minimize localized biofilm acidification due to shorter ion transport distances while back diffusion of anions in the cathode chamber was minimized by charge repulsion and the electrons flowing from the anode to the cathode. In contrast to the AEM, the CEM and UFM allow for sodium and potassium ion transport from the anolyte through the membrane and into the cathode.[15,24,26] This ion transport will not help to balance pH and can lead to salt precipitation in the cathode.[27] In addition to demonstrating the importance of the AEM as a critical factor in high power the cathode performance was further improved by using an iron-phthalocyanine (Fe-Pc) catalyst to increase the cell potential.[28–30]

2. Materials and methods

2.1. Construction and operation of the MFCs

The MFCs were constructed with two chambers each with HDPE endplates and silicon gaskets (7 cm^2 exposed electrode area) (Fig. 2). The chambers were separated only by an AEM (106 μm thick with an ion exchange capacity of 1.85 mmol g^{-1}, Selemion AMV-N, Asahi Glass, Co., Tokyo, Japan) to promote hydroxide ion transport away from the

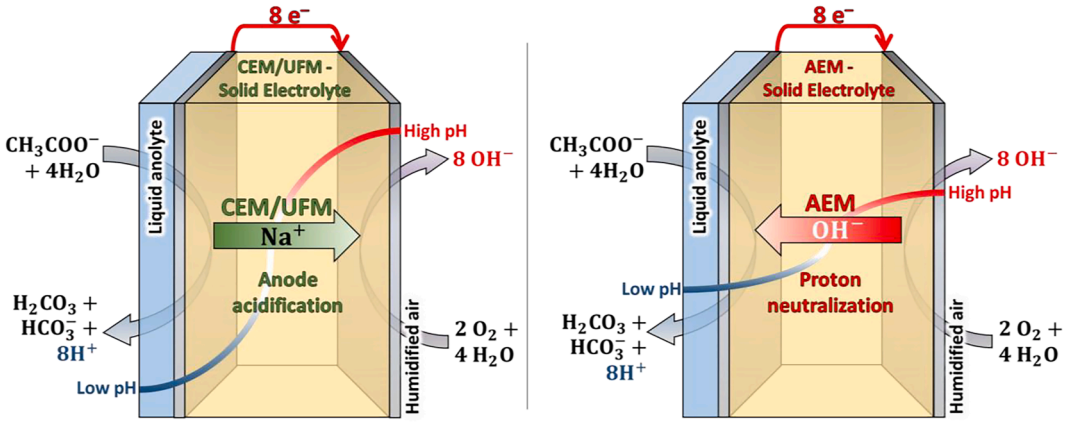

Fig. 1. Schematic of the transport of chemicals in the zero-gap MFC with an (A) AEM and (B) CEM or UFM. Note that no catholyte is present, and only the hydroxide ions from the ORR can balance charge transport in the AEM-MFC configuration while the positive ions in the anode chamber are preferentially transported in the CEM/UFM configuration, leading to larger pH differences between anode and cathode.

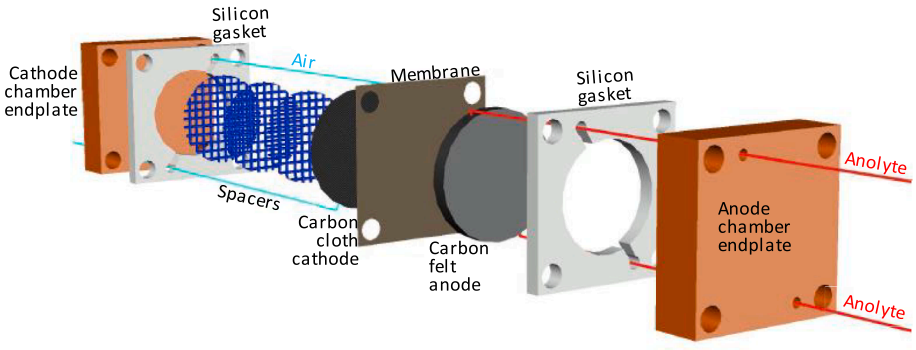

Fig. 2. Exploded view of the MFC configuration used in this study.

cathode. Two other membranes were used as controls. A CEM (183 μm thick, Nafion 117, Chemours) was used to selectively transport cations, or a UF membrane (DIAFLO PM-10 polysulfone membrane, molecular weight cutoff 10,000 Daltons) that was not ion-selective.

The anode chamber was completely occupied by the carbon felt anode (7 cm^2 projected area, 3.18 mm thick, Alfa Aesar) that was heat treated at 450°C for 30 min before being used to increase the electroactive surface area.[31] The anode was inoculated with MFC effluent from other operating reactors and acclimated in a 4 cm cubic MFC at a constant potential of + 200 mV for more than two weeks prior to be transferred in the flow cell. Acclimation at + 200 mV have previously showed to improve current production and increase the biofilm mass and concentrations of exoelectrogens such as *Geobacter* spp.[32]

The cathode catalyst was iron-phtalocyanine Fe-Pc (Alfa-Aesar) dispersed in carbon black (Vulcan XC 72) sprayed on hydrophilic carbon cloth (Fuel Cell Store) with four additional layers of PTFE as previously described[33] (final loading of 7.5 mg cm^{-2}). The ionomer used in the cathode was quaternary 1,4-diazabicyclo-[2.2.2]-octane (DABCO) polysulphone (QDPSU) dispersed in dimethylacetamide and sonicated with the catalyst in an optimized 1:10 ratio for one hour in ice before spraying it on the carbon cloth. The Fe-Pc cathode was compared with a Pt/C cathode prepared as previously described.[22] Nafion (5% in low aliphatic alcohol, Sigma Aldrich) was used as ionomer in the CEM configuration with a catalyst to ionomer ratio of 1:10. Cathodes and AEMs or UFM were cold-pressed together at 4500 psi for 10 min, while cathodes and CEMs were hot-pressed at 1000 psi and 130°C for 1 min to produce the membrane electrode assembly (MEA) used in the MFC. The cathode catalyst layer morphology and atomic composition was characterized using scanning electron microscopy in conjunction with energy dispersive X-ray spectroscopy (SEM-EDX). The anode felt and the cathode catalyst layer were analyzed after disassembling the MFCs with the SEM-EDX and the ESEM. Prior to MFC assembly three layers of plastic mesh spacers (S1.5, 30PTFE-625P, Dexmet Corp.) were inserted between the cathode and the endplate in the cathode chamber to maintain a zero-gap spacing between the electrodes while allowing air to flow past the cathode. Titanium foils (Strem Chemicals Inc.) were used as anode and cathode current collectors.

The anolyte (500 mL) was recirculated in the anode chamber at a flow rate of 10 mL min^{-1} (theoretical hydraulic retention time of HRT = 13.4 s) while only humidified air was pumped past the cathode at 2.5 mL min^{-1} (HRT = 53 s). The high flow rate in our system was used to minimize concentration boundary layers due to substrate consumption. The anolyte was a 50 mM phosphate buffer (PBS, 4.58 g L^{-1} Na_2HPO_4, 2.45 g L^{-1} NaH_2PO_4 H_2O, 0.31 g L^{-1} NH_4Cl, 0.13 g L^{-1} KCl) at pH 7.0 with a solution conductivity of 6.93 mS cm^{-1}. Sodium acetate was added as the substrate (2 g L^{-1}), and the medium was amended with trace vitamin and mineral solutions before feeding to the reactor.[34] We used 50 mM PBS and sodium acetate to allow a comparison of our results with the existing MFC literature, where sodium acetate in PBS 50 mM has been extensively used.[35] Lower performance would have been obtained with real waste streams such as domestic wastewater; however, the variable composition of wastewater would not have allowed a fair comparison with the literature, and the reproducibility of our results by others. Duplicate MFCs were fed daily and operated in a temperature-controlled room at 30°C. Unfortunately, the compact MFC configuration did not allow to measure the individual anode and cathode potentials against a reference, which is desired to better monitor the individual contributions of the electrodes to the overall internal resistance.[36] Thus, due to the configuration used here only the whole cell voltage was monitored.

2.2. Electrochemical measurements

The MFC voltage was recorded with an automatic data acquisition system (Keithley 2700). The MFCs were connected to a 10 Ω external resistance and the current (i) and power (P) were calculated using Ohm's law as I = V/R and P = I/V. Current density (I) and power density (PD) were obtained by normalizing the current and the power by the cross-sectional area of the electroactive region (7 cm^2). Prior to assembly the cell the anode and cathode electrochemical performance were investigated with linear sweep voltammetry (LSV) in three electrode configuration using and Ag/AgCl reference electrode (single junction silver chloride (Ag/AgCl) reference electrode; model RREF0021, Pine Research Instrumentation, NC; + 199 mV versus a standard hydrogen electrode, SHE) and IR corrected for the ohmic drop. The solution resistance (R_Ω) was calculated with electrochemical impedance spectroscopy (EIS) by conducting a fast EIS (from 100 kHz to 500 Hz, 5 mV amplitude, 10 points s^{-1}, ≈25 s $scan^{-1}$).[37] The whole cell and the individual electrode performance were analyzed with the electrode potential slope (EPS) method.[17]

Single cycle polarization tests were conducted on the flow-MFCs by applying a variable external resistance (1000, 500, 200, 100, 75, 50, 30, 20, 10, 5, 3 Ω) at 20 min intervals after feeding the reactors with fresh solution and leaving the cell in open circuit for 2 h. The voltage drop (U) across the external resistor was recorded by a computer-based data acquisition system (VMP3, Bio-logic, France). All potentials are reported here versus SHE.

3. Results and discussion

3.1. Impact of charge transfer through the membrane on MFC performance

Based on polarization tests the MFC with the AEM produced a maximum power density of 8.8 ± 0.5 W m^{-2} (Fig. 3). This power density was around three times larger than that produced using the CEM (3.1 ± 0.1 W m^{-2}), or a non-ion selective UFM (2.4 ± 0.1 W m^{-2}). The AEM-MFC internal resistance was 5.0 ± 0.1 mΩ m^2, which was more than 50% lower than that of the two other configurations which had internal resistances of R_{int} = 12 ± 1 mΩ m^2 (CEM-MFC) and R_{int} = 14.8 ± 0.8 mΩ

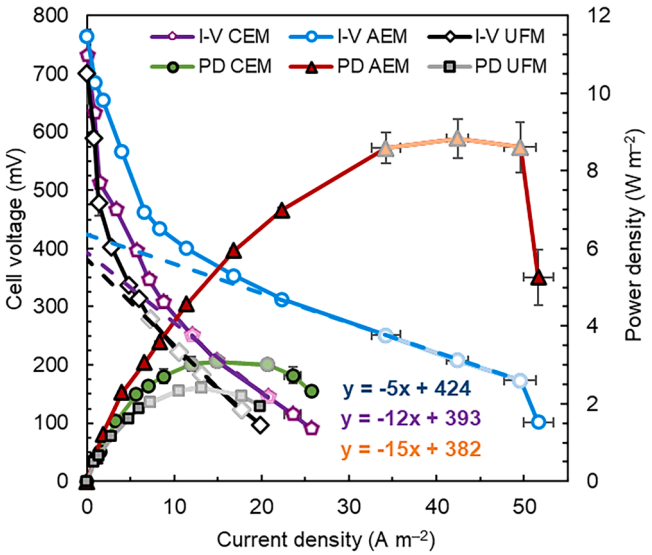

Fig. 3. Performance of the MFCs with an AEM, CEM or UFM membranes in polarization tests. The dashed lines represent the linearization of the data in the maximum power region (faded).

m^2 (UFM-MFC). The maximum power density in the polarization tests using the AEM as solid electrolyte was the highest power density ever reported for MFCs using 50 mM PBS and acetate. In addition, this power density exceeded those produced using higher buffer concentrations of up to 200 mM PBS or other solutions used to increase conductivities and buffer capacities of the electrolytes. The power density reported in this study was 50% larger than the highest power density reported to date of 5.9 ± 0.5 W m^{-2}, although with an higher buffer concentration (70 mM phosphate/carbonate), with higher conductivity (12.5 mS cm^{-1} vs 6.93 mS cm^{-1} used here) and at an higher temperature (35°C compared to 30°C) than that used here.[21,38,39] The flow rates and the cathode catalysts were the same for the AEM-, CEM- and UFM-MFCs, thus, the large difference in maximum power density was not due to the flow rates or different catalyst material, but instead to the control of hydroxide ion transport.

The AEM-MFC internal resistance was 58% lower than the CEM-MFC R_{int} due to the selective transport of hydroxide ions from the cathode to the anode, limiting the acidification of the biofilm. The MFC internal resistance is a combination of the solution/membrane (R_Ω), cathode (R_{Cat}), and anode (R_{An}) resistances. Limiting the biofilm acidification by transporting the hydroxide ions directly into the biofilm could decrease the anode resistance, which is a combination of charge transfer and proton diffusion resistances.[17] The solution resistance arises from the low conductivity of the electrolyte separating the electrodes, and thus limits current generation due to the resistance in the transport of ions that is needed to balance the movement of the electrons from anode to cathode. The solution resistance is only a function of the reactor configuration and specific membrane, and it was 26% of the overall internal resistance for the AEM-MFC (R_Ω = 1.3 ± 0.1 mΩ m^2) and only 8% for the CEM-MFC (R_Ω = 0.95 ± 0.04 mΩ m^2) and 21% for the UFM-MFC (R_Ω = 3.1 ± 0.5 mΩ m^2), indicating that the membrane resistances were all small and therefore that differences in membrane resistance were not responsible for the very large differences in maximum power densities obtained using the different membranes.

The cathode and the anode resistances are a combination of the charge transfer (kinetic) and diffusion (mass-transport) processes occurring at the correspondent electrode.[19] The ORR kinetic is the only contributor to R_{Cat} in the current density range typical for MFCs (<100 A m^{-2}), which is much lower than that of fuel cells (greater than 1 A cm^{-2}), where diffusion limitations can occur.[19,40] Instead, the diffusion resistance in the transport of protons from the anode plays a major role in R_{An}, by limiting the activity of the exoelectrogenic microorganisms through the acidification of the biofilm.[11,19,20] While previous studies have shown slightly better performance using AEMs in bioelectrochemical systems compared to CEM or unselective membranes, these studies were all conducted using two chambers, each containing liquid electrolytes.[41,42] The presence of negative ions in the catholyte and their larger concentration compared to the hydroxide ions at pH 7 (0.1 μM) favor the migration of ions other than OH^- under the effect of the electric field, leading to large pH imbalances between the two electrodes.[15] The maximum power density was previously reported to increase by more than 40% when a CEM was replaced with an AEM (AEM = 0.1 W m^{-2}; CEM = 0.07 W m^{-2})[43], however, such power densities were only 1% of those reported here, suggesting that using an AEM alone does not enable larger power production. The AEM needs to be used in combination with a small electrode spacing and the absence of a catholyte, in order to have only the hydroxide ions at the cathode, and a small spacing between where the OH^- are generated and where they are neutralized by the protons.

3.2. Stability of MFC performance

Maintaining stable performance at a high power output is essential for application of MFCs, and therefore the maximum power should be maintained and not rapidly decrease over relatively short periods of time as shown in some previous studies.[27,38,44] The AEM-MFC produced a stable output for over seven days of continuous operation, with a peak power density of 8.36 ± 0.02 W m^{-2} for day 2 (10 Ω external resistance), with only a minor decrease of <4% by day 7 (8.06 ± 0.01 W m^{-2}) (Fig. 4). The power density produced over seven days of operation with a 10 Ω external resistance was similar to the power density obtained in polarization test with the same resistance (8.6 ± 0.4 W m^{-2}), showing that the performance obtained in the polarization test were representative of the MFC performance under continuous operations. In contrast, the CEM-MFC performance decreased by 9% and the UFM-MFC by 12% over the same period likely due to the transport of positively charged ions into the cathode. This transport of cations, coupled with the high local pH due to the ORR, would be expected to result in precipitation of salts within the cathode structure. EDX analysis of the

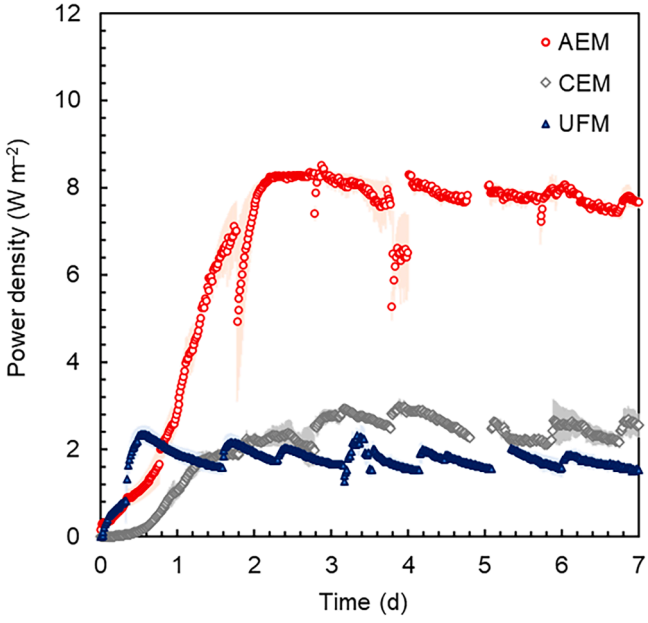

Fig. 4. Performance of the MFCs with an AEM, CEM or UFM membranes over time during the first week of operation. At day 4 the external resistance of the AEM-MFC was decreased to 5 Ω for 6 h, then returned to 10 Ω. The polarization tests were conducted for all the configurations at day 5.

membrane side of the MEA cathodes at the end of the experimental phase confirmed the importance of cation transport into the cathode. The mass of cations such as Na and Mg were increased in the CEM- and UFM-MFCs but not in the AEM-MFCs. In addition, only a small amount of P and Cl atoms were identified in the AEM-MFC. The different accumulation of these ions indicated that the AEM-MFC was effective in transport of hydroxide ions from the cathode to the anode, while CEM and UFM primarily transferred positive ions other than protons to the cathode. Previous studies have failed in showing high and stable performance, for example, the maximum power density decreased by 19% after only two days of operation in a previous study reporting a high power density of 5.9 ± 0.5 W m^{-2}.[38] The authors suggested that the fast decrease in the performance was due to the cathode fouling that limited the MFC performance mainly by the precipitation of salts within the catalyst layer structure.[27] The salts diminished the accessibility and thus activity of the catalytic sites, and could have decreased the conductivity of the carbonaceous matrix of the electrode.[27,44] The use of an AEM here limited the transport of cations toward the cathode, and the transport of negative ions in the same direction is hindered by the electron flow, from anode to cathode, thus avoiding either salt precipitation and allowing a better control of the local cathode pH. Unlike in previous two-chamber MFC tests with either AEM or CEMs where the anolyte pH decreased and the catholyte pH increased,[24] the anolyte pH here was stable throughout the experiments within a narrow range of 6.9–7.2.

Pumping air at a controlled flow rate coupled with a membrane separating anode and cathode limited the intrusion of oxygen in the anode chamber, increasing the Coulombic efficiency (CE) for all the configuration tested. The AEM-MFC CE averaged 102 ± 15% over three different cycles while the CEM-MFC was 90 ± 5% and the UFM-MFC was 81 ± 20%. Pumping humidified air past the cathode can increase the energy required to operate our MFC. However, previous studies have suggested that the power consumed to pump air into a cathode chamber is only 0.1 W m^{-2},[45] thus, it can be easily offset by the high power density produced in the configuration used here. The COD removal of the AEM-MFC was 22 ± 3%, around two times that obtained in the CEM- and UFM-MFC configurations (10 ± 1%), likely due to the larger current density of the AEM-MFC compared to CEM- and UFM-MFCs.

3.3. Comparison of the individual electrodes with the assembled AEM-MFC

The selective transport of hydroxide ions across the AEM boosted the individual anode and cathode performance, as can be seen by a comparison of the individual electrode LSVs in separate tests, with the assembled AEM-MFC (Fig. 5). When the bioanode performance was tested separately in a three-electrode configuration typical of MFCs (i.e. with no stirring), the peak current density was 8.9 ± 0.8 A m^{-2}. This current density was 6 times smaller than the current density of the assembled AEM-MFC in polarization tests (52 ± 2 A m^{-2}), using the exact same electrode. This much improved performance of the anode in the AEM-MFC suggests that the hydroxide ions, generated at the cathode from the ORR, effectively migrated to the anode chamber through the AEM in the assembled configuration, avoiding the biofilm acidification and allowing production of larger current densities. In a typical cubic configuration, however, other ions present in solution that were more concentrated than H^+ and OH^- maintain charge balance developing differential pH between anode and cathode.[15,20] The acidification of the biofilm on the anode has previously been suggested to limit the maximum current densities deliverable by bioanodes.[11,20] For example, it was shown that the anode limiting current density and the buffer concentration in solution follow a linear relationship, and that a high buffer concentration allowed generation of larger current densities by better controlling the localized pH near the anode.[11]

Effective removal of hydroxide ions produced by the ORR at the cathode increased the cell voltage (Fig. 5). The cathode, unlike the anode, did not show any limiting current density in LSVs as the ORR can occur over the whole range of pHs. However, the solution pH can still reduce the electrode potential by up to 59 mV based on calculations using the Nernst equation.[19] The cathode experimental potential measured using LSVs in the same three-electrode configuration used for the anode, was only 82 ± 2 mV based on extrapolation using the current density range near the maximum power (35–50 A m^{-2}). This potential was 342 mV lower than that obtained from the whole AEM-MFC (both electrodes) in the same current density range. The anode open circuit potential (OCP) was –251.1 ± 0.1 mV which by itself could not account for the large difference between the cathode potential and the whole cell voltage as the difference between anode and cathode potentials represent the overall cell voltage. Thus, the AEM-MFC configuration facilitated more efficient hydroxide ion transport which decreased the pH hear the cathode, and increased the cathode potential. The effective ion transport was enabled by the use of a thin catalyst layer (40 μm, Fig. 6B) tightly pressed against the AEM.

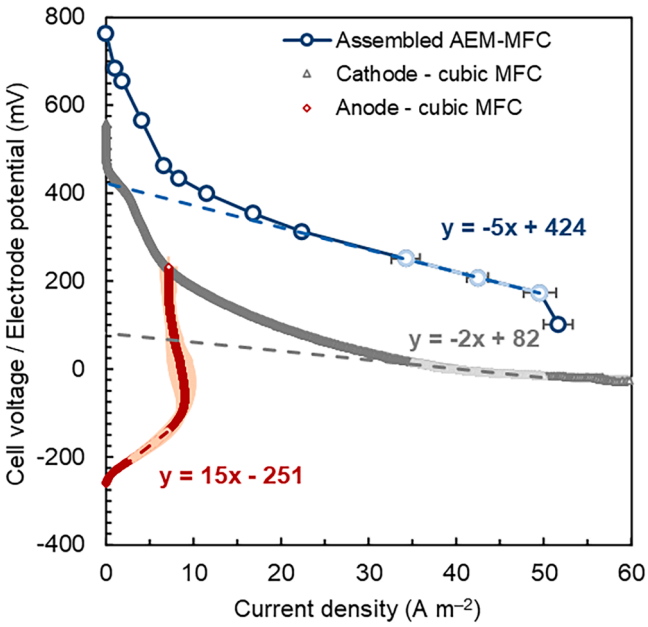

Fig. 5. Comparison of the individual anode and cathode performance with LSVs and overall cell potential from polarization test. Anode and cathode potentials were corrected for the ohmic drop.

The cathode performance was improved here by using a Fe-Pc catalyst compared to a Pt/C cathode (Fig. 6).[17] The cathode experimental potential measured in a cubic MFC over a current density range of 35–50 A m^{-2} was 88 mV larger than that of a cathode with Pt catalyst (0.5 mg cm^{-2}) (Supporting Information). Such a potential gain may appear not to be that important compared to the electrode OCP (551 ± 6 mV), but the total voltage gained at the current density at maximum power production (42 ± 1 A m^{-2}) represents an addition of 3.7 W m^{-2} in the whole cell. Moreover, Fe-N-C catalysts are less susceptible to poisoning in the complex media typical for MFCs.[44,46] For example, the maximum power density of MFCs with Fe-N-C based catalyst decreased by 10% during the first ten days of operation (from 2.0 ± 0.0 W m^{-2} to 1.8 ± 0.0 W m^{-2}), compared to an overall decrease of 28% of a Pt-based catalyst (from 1.7 ± 0.0 W m^{-2} to 1.2 ± 0.0 W m^{-2}).[44] Thus, the high stability of Fe-N-C catalyst allowed the negligible decrease (<4%) in power production observed in this study.

3.4. Outlook

The maximum power density of 8.8 ± 0.5 W m^{-2} in the AEM-MFC obtained here represents a new milestone in MFC performance that was made possible by the improved architecture that lowered internal

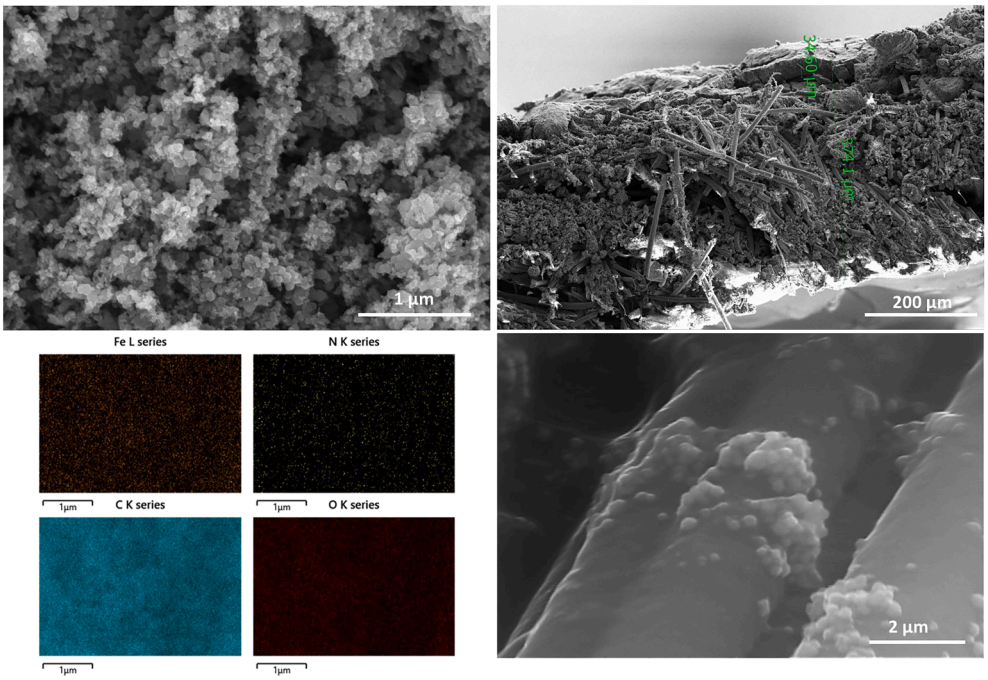

Fig. 6. SEM images of the (A, B) Fe-Pc derived catalyst at different magnifications and (C) correspondent EDX mapping for the Fe, N and C distribution. (D) ESEM image of the biofilm on the carbon felt anode.

resistance, and the use of the Fe-Pc cathode catalyst. This high power density has not been obtained using previous methods to reduce internal resistance, such as increasing the solution conductivity or buffer capacity, or only reduce the electrode spacing.[15,47] Here, by using the AEM to separate anode and cathode, not having any catholyte, and using closely spaced electrodes allowed the hydroxide ions generated by the ORR at the cathode to be effectively transferred to the anode with the aid of the electric field. This AEM configuration avoided development of high pH differences between the electrodes, boosted the anode current density and increased the cathode electrode potential. When a CEM or UFM was used instead of the AEM, Na and Mg were preferentially transported through the membrane compared to hydroxide ions, causing the acidification of the anode biofilm and an increase in the pH next to the cathode which in turn increased the electrode overpotentials and decreased the maximum current. Unfortunately, the use of an AEM increases the cost of the MFC materials. The cost of AEMs ranges from \$100–\$1000 m^{-2} (\$268 m^{-2} for the AEM used here). However, it may be possible do develop less expensive membranes or cathode coatings. The higher performance of the AEM-MFC, coupled with the longer stability of the reactor, could provide a trade-off for the higher capital costs of this reactor configuration.

Treating real waste streams with high content of dispersed solids can be challenging in compact MFC structures like the one used in this study. The porous carbon felt can act as a filter and accumulate the solids in the wastewaters, clogging the MFC. However, solids can be removed from the wastewater through filtration or centrifugation, or less-compact structure can be developed for treating these waste streams. For example, it was recently shown that a zero-gap MFC can treat streams with solid contents up to 360 mg L^{-1} using spacers placed between the anode and the end plate, to increase the void volume of the MFC while allowing a close contact between the anode and the AEM, to avoid biofilm acidification.[48]

Further increases in the MFC performance could still be possible. The AEM was effective in favoring transport of the hydroxide ions from the cathode to the anode chamber, but not through the carbon felt anode inner porosity. Researchers have tried to identify the optimal porosities of the carbon structures used for bioanodes, showing that the acidification of the biofilm in the pores is largely controlled by the buffer capacity of the solution.[9,49] A large pH drop (0.4 unit of pH) was observed along the biofilm when the phosphate buffer concentration was lowered from 100 mM to 50 mM, causing damage to the bacteria in the 40 µm inner layer of the bioanodes.[50] Thus, to mitigate local acidification of the anode biofilm, hydroxide ions should be transported not only into the anode chamber, but also more effectively into the anode pores. The transport of chemical species is favored in electrodes for fuel cells by dispersing an ion selective polymer in the catalyst matrix. While doping a microbial biofilm with anion exchange ionomers (AEI) would be challenging due to the low biocompatibility of the solvents, higher current densities were obtained in the past by coating electrode with an AEI before biofilm cultivation.[51] For example, a graphite granule anode doped with DABCO, the same ionomer used here in the cathode, produced a current density (116 A m^{-3}) that was six times higher than that of an unmodified electrode.[51]

Increasing the biofilm conductivity could further increase the MFC performance. Doping an anodic biofilm with copper sulfide has recently been shown to increase the conductivity of the bioanode and produce larger current densities.[52] The electrode in that study was cultivated in a three electrode configuration with copper sulfide in solution (in complete absence of oxygen) and produced 237% more current than the undoped anode (maximum of 16 ± 2 A m^{-2}, compared to 42 ± 1 A m^{-2} at maximum power point here).[52] Here, we demonstrated that improving the hydroxide ion management and limiting the biofilm acidification in the AEM-MFC allowed the maximum power density to increase by 184% compared to the CEM-MFC (286% increase in current density at maximum power point) and by 267% compared to the UFM-MFC (324% increase in current density at maximum power point). Thus, through ion management, biofilm acidification and MFC configurations played a more critical role in the determination of the MFC performance than biofilm conductivity. Furthermore, methods such as increasing solution conductivity and using higher buffer concentrations, could improve the anode performance, and cathodes with higher reduction potentials could further improve electrode and whole cell performance using this AEM-MFC design.

4. Conclusions

The zero-gap MFC with AEM produced the highest maximum power density ever reported in the literature of 8.8 ± 0.5 W m^{-2} (at 42 ± 1 A m^{-2}). The selectivity of the hydroxide transport across the AEM with no catholyte enabled the high MFC performance, limiting biofilm acidification by neutralizing the protons produced at the anode and boosting the maximum current and power densities. When the AEM was replaced with a CEM or a UFM the maximum current and power densities drastically decreased due to the enabling transport of cations such as sodium and magnesium to the cathode for balancing charge. The SEM analysis showed a lack of cation transport into the cathode using an AEM that avoided salt precipitation in the cathode, and thus enabling more stable power production over time.

Declaration of Competing Interest

The authors declare that they have no known competing financial interests or personal relationships that could have appeared to influence the work reported in this paper.

Acknowledgements

The authors acknowledge funding by the Environmental Security Technology Certification Program via cooperative research agreement W9132T-16-2-0014 through the US Army Engineer Research and Development Center and Penn State University.

Appendix A. Supplementary data

Supplementary data to this article can be found online at https://doi.org/10.1016/j.cej.2021.130150.

References

[1] B.E. Logan, B. Hamelers, R. Rozendal, U. Schröder, J. Keller, S. Freguia, P. Aelterman, W. Verstraete, K. Rabaey, Microbial fuel cells: Methodology and technology, Environ. Sci. Technol. 40 (2006) 5181–5192, https://doi.org/10.1021/es0605016.

[2] D. Pocaznoi, B. Erable, M.-L. Delia, A. Bergel, Ultra microelectrodes increase the current density provided by electroactive biofilms by improving their electron transport ability, Energy Environ. Sci. 5 (1) (2012) 5287–5296, https://doi.org/10.1039/C1EE01469B.

[3] B.E. Logan, R. Rossi, A. Ragab, P.E. Saikaly, Electroactive microorganisms in bioelectrochemical systems, Nat. Rev. Microbiol. 17 (5) (2019) 307–319, https://doi.org/10.1038/s41579-019-0173-x.

[4] B. Liang, Y. Zhao, M. Zong, S. Huo, I.U. Khan, K. Li, C. Lv, Hierarchically porous N-doped carbon encapsulating CoO/MgO as superior cathode catalyst for microbial fuel cell, Chem. Eng. J. 385 (2020) 123861, https://doi.org/10.1016/j.cej.2019.123861.

[5] D. Massazza, R. Parra, J.P. Busalmen, H.E. Romeo, New ceramic electrodes allow reaching the target current density in bioelectrochemical systems, Energy Environ. Sci. 8 (9) (2015) 2707–2712, https://doi.org/10.1039/C5EE01498K.

[6] V. Flexer, J. Chen, B.C. Donose, P. Sherrell, G.G. Wallace, J. Keller, The nanostructure of three-dimensional scaffolds enhances the current density of microbial bioelectrochemical systems, Energy Environ. Sci. 6 (2013) 1291–1298, https://doi.org/10.1039/c3ee00052d.

[7] S. Chen, G. He, Q. Liu, F. Harnisch, Y. Zhou, Y. Chen, M. Hanif, S. Wang, X. Peng, H. Hou, U. Schröder, Layered corrugated electrode macrostructures boost microbial bioelectrocatalysis, Energy Environ. Sci. 5 (2012) 9769–9772, https://doi.org/10.1039/c2ee23344d.

[8] Y. Li, J. Liu, X. Chen, X. Yuan, N. Li, W. He, Y. Feng, Enhanced electricity generation and extracellular electron transfer by polydopamine–reduced graphene oxide (PDA–rGO) modification for high-performance anode in microbial fuel cell, Chem. Eng. J. 387 (2020) 123408, https://doi.org/10.1016/j.cej.2019.123408.

[9] P. Chong, B. Erable, A. Bergel, Effect of pore size on the current produced by 3-dimensional porous microbial anodes: A critical review, Bioresour. Technol. 289 (2019) 121641, https://doi.org/10.1016/j.biortech.2019.121641.

[10] J. Kretzschmar, S. Riedl, R.K. Brown, U. Schröder, F. Harnisch, eLatrine: Lessons learned from the development of a low-tech MFC based on cardboard electrodes for the treatment of human feces, J. Electrochem. Soc. 164 (3) (2017) H3065–H3072, https://doi.org/10.1149/2.0121703jes.

[11] C.I. Torres, A. Kato Marcus, B.E. Rittmann, Proton transport inside the biofilm limits electrical current generation by anode-respiring bacteria, Biotechnol. Bioeng. 100 (5) (2008) 872–881, https://doi.org/10.1002/bit.v100:510.1002/bit.21821.

[12] S. Gadkari, J.-M. Fontmorin, E. Yu, J. Sadhukhan, Influence of temperature and other system parameters on microbial fuel cell performance: Numerical and experimental investigation, Chem. Eng. J. 388 (2020) 124176, https://doi.org/10.1016/j.cej.2020.124176.

[13] W. Yang, X.u. Wang, R. Rossi, B.E. Logan, Low-cost Fe–N–C catalyst derived from Fe (III)-chitosan hydrogel to enhance power production in microbial fuel cells, Chem. Eng. J. 380 (2020) 122522, https://doi.org/10.1016/j.cej.2019.122522.

[14] K. Lawson, R. Rossi, J.M. Regan, B.E. Logan, Impact of cathodic electron acceptor on microbial fuel cell internal resistance, Bioresour. Technol. 316 (2020) 123919, https://doi.org/10.1016/j.biortech.2020.123919.

[15] M. Oliot, S. Galier, H. Roux de Balmann, A. Bergel, Ion transport in microbial fuel cells: Key roles, theory and critical review, Appl. Energy. 183 (2016) 1682–1704, https://doi.org/10.1016/j.apenergy.2016.09.043.

[16] R. Rossi, B.E. Logan, Unraveling the contributions of internal resistance components in two-chamber microbial fuel cells using the electrode potential slope analysis, Electrochim. Acta. 348 (2020) 136291, https://doi.org/10.1016/j.electacta.2020.136291.

[17] R. Rossi, B.P. Cario, C. Santoro, W. Yang, P.E. Saikaly, B.E. Logan, Evaluation of electrode and solution area-based resistances enables quantitative comparisons of factors impacting microbial fuel cell performance, Environ. Sci. Technol. 53 (7) (2019) 3977–3986, https://doi.org/10.1021/acs.est.8b0600410.1021/acs.est.8b06004.s001.

[18] R. Rossi, D. Pant, B.E. Logan, Chronoamperometry and linear sweep voltammetry reveals the adverse impact of high carbonate buffer concentrations on anode performance in microbial fuel cells, J. Power Sources. 476 (2020) 228715, https://doi.org/10.1016/j.jpowsour.2020.228715.

[19] R. Rossi, D.M. Hall, X.u. Wang, J.M. Regan, B.E. Logan, Quantifying the factors limiting performance and rates in microbial fuel cells using the electrode potential slope analysis combined with electrical impedance spectroscopy, Electrochim. Acta. 348 (2020) 136330, https://doi.org/10.1016/j.electacta.2020.136330.

[20] S.C. Popat, C.I. Torres, Critical transport rates that limit the performance of microbial electrochemistry technologies, Bioresour. Technol. 215 (2016) 265–273, https://doi.org/10.1016/j.biortech.2016.04.136.

[21] W. Yang, B.E. Logan, Immobilization of a metal-nitrogen-carbon catalyst on activated carbon with enhanced cathode performance in microbial fuel cells, ChemSusChem 9 (16) (2016) 2226–2232, https://doi.org/10.1002/cssc.201600573.

[22] R. Rossi, X.u. Wang, B.E. Logan, High performance flow through microbial fuel cells with anion exchange membrane, J. Power Sources. 475 (2020) 228633, https://doi.org/10.1016/j.jpowsour.2020.228633.

[23] S.C. Popat, D. Ki, B.E. Rittmann, C.I. Torres, Importance of OH^- transport from cathodes in microbial fuel cells, ChemSusChem. 5 (6) (2012) 1071–1079, https://doi.org/10.1002/cssc.v5.610.1002/cssc.201100777.

[24] R.A. Rozendal, H.V.M. Hamelers, C.J.N. Buisman, Effects of membrane cation transport on pH and microbial fuel cell performance, Environ. Sci. Technol. 40 (17) (2006) 5206–5211, https://doi.org/10.1021/es060387r10.1021/es060387r.s001.

[25] A.W. Jeremiasse, H.V.M. Hamelers, M. Saakes, C.J.N. Buisman, Ni foam cathode enables high volumetric H_2 production in a microbial electrolysis cell, Int. J. Hydrogen Energy. 35 (23) (2010) 12716–12723, https://doi.org/10.1016/j.ijhydene.2010.08.131.

[26] F. Zhao, F. Harnisch, U. Schröder, F. Scholz, P. Bogdanoff, I. Herrmann, U. Schroder, Challenges and constraints of using oxygen cathodes in microbial fuel cells, Environ. Sci. Technol. 40 (2006) 5193–5199, https://doi.org/10.1021/es060332p\nhttp://www.ncbi.nlm.nih.gov/pubmed/16999088.

[27] J. An, N. Li, L. Wan, L. Zhou, Q. Du, T. Li, X. Wang, Electric field induced salt precipitation into activated carbon air-cathode causes power decay in microbial fuel cells, Water Res. 123 (2017) 369–377, https://doi.org/10.1016/j.watres.2017.06.087.

[28] F. Zhao, F. Harnisch, U. Schröder, F. Scholz, P. Bogdanoff, I. Herrmann, Application of pyrolysed iron(II) phthalocyanine and CoTMPP based oxygen reduction catalysts as cathode materials in microbial fuel cells, Electrochem. Commun. 7 (12) (2005) 1405–1410, https://doi.org/10.1016/j.elecom.2005.09.032.

[29] J. Ahmed, Y. Yuan, L. Zhou, S. Kim, Carbon supported cobalt oxide nanoparticles-iron phthalocyanine as alternative cathode catalyst for oxygen reduction in microbial fuel cells, J. Power Sources. 208 (2012) 170–175, https://doi.org/10.1016/j.jpowsour.2012.02.005.

[30] A. Iannaci, B. Mecheri, A. D'Epifanio, M.J. Lázaro Elorri, S. Licoccia, Iron–nitrogen-functionalized carbon as efficient oxygen reduction reaction electrocatalyst in microbial fuel cells, Int. J. Hydrogen Energy. 41 (43) (2016) 19637–19644, https://doi.org/10.1016/j.ijhydene.2016.04.154.

[31] Y. Feng, Q. Yang, X. Wang, B.E. Logan, Treatment of carbon fiber brush anodes for improving power generation in air-cathode microbial fuel cells, J. Power Sources. 195 (7) (2010) 1841–1844, https://doi.org/10.1016/j.jpowsour.2009.10.030.

[32] X. Zhu, M.D. Yates, M.C. Hatzell, H. Ananda Rao, P.E. Saikaly, B.E. Logan, Microbial community composition is unaffected by anode potential, Environ. Sci. Technol. 48 (2) (2014) 1352–1358, https://doi.org/10.1021/es404690q.

[33] S. Cheng, H. Liu, B.E. Logan, Increased performance of single-chamber microbial fuel cells using an improved cathode structure, Electrochem. Commun. 8 (3) (2006) 489–494, https://doi.org/10.1016/j.elecom.2006.01.010.

[34] S. Cheng, D. Xing, D.F. Call, B.E. Logan, Direct biological conversion of electrical current into methane by electromethanogenesis, Environ. Sci. Technol. 43 (10) (2009) 3953–3958, https://doi.org/10.1021/es803531g.

[35] W. Yang, K.-Y. Kim, P.E. Saikaly, B.E. Logan, The impact of new cathode materials relative to baseline performance of microbial fuel cells all with the same architecture and solution chemistry, Energy Environ. Sci. 10 (5) (2017) 1025–1033, https://doi.org/10.1039/C7EE00910K.
[36] F. Zhang, J. Liu, I. Ivanov, M.C. Hatzell, W. Yang, Y. Ahn, B.E. Logan, Reference and counter electrode positions affect electrochemical characterization of bioanodes in different bioelectrochemical systems, Biotechnol. Bioeng. 111 (10) (2014) 1931–1939, https://doi.org/10.1002/bit.25253.
[37] B.E. Logan, E. Zikmund, W. Yang, R. Rossi, K.-Y. Kim, P.E. Saikaly, F. Zhang, Impact of ohmic resistance on measured electrode potentials and maximum power production in microbial fuel cells, Environ. Sci. Technol. 52 (15) (2018) 8977–8985, https://doi.org/10.1021/acs.est.8b0205510.1021/acs.est.8b02055.s001.
[38] M. Oliot, L. Etcheverry, A. Mosdale, R. Basseguy, M.L. Délia, A. Bergel, Separator electrode assembly (SEA) with 3-dimensional bioanode and removable air-cathode boosts microbial fuel cell performance, J. Power Sources. 356 (2017) 389–399, https://doi.org/10.1016/j.jpowsour.2017.03.016.
[39] Y. Fan, S.K. Han, H. Liu, Improved performance of CEA microbial fuel cells with increased reactor size, Energy Environ. Sci. 5 (2012) 8273–8280, https://doi.org/10.1039/c2ee21964f.
[40] F. Yin, P. Hu, C. Song, S. Wang, H. Liu, Unveiling the role of gas permeability in air cathodes and performance enhancement by waterproof membrane fabricating method, J. Power Sources. 449 (2020) 227570, https://doi.org/10.1016/j.jpowsour.2019.227570.
[41] T.H.J.A. Sleutels, A. terHeijne, P. Kuntke, C.J.N. Buisman, H.V.M. Hamelers, Membrane selectivity determines energetic losses for ion transport in bioelectrochemical systems, ChemistrySelect. 2 (12) (2017) 3462–3470, https://doi.org/10.1002/slct.201700064.
[42] T.H.J.A. Sleutels, H.V.M. Hamelers, R.A. Rozendal, C.J.N. Buisman, Ion transport resistance in microbial electrolysis cells with anion and cation exchange membranes, Int. J. Hydrogen Energy. 34 (9) (2009) 3612–3620, https://doi.org/10.1016/j.ijhydene.2009.03.004.
[43] H.-C. Tao, X.-N. Sun, Y. Xiong, A novel hybrid anion exchange membrane for high performance microbial fuel cells, RSC Adv. 5 (6) (2015) 4659–4663, https://doi.org/10.1039/C4RA11638K.
[44] C. Santoro, A. Serov, L. Stariha, M. Kodali, J. Gordon, S. Babanova, O. Bretschger, K. Artyushkova, P. Atanassov, Iron based catalysts from novel low-cost organic precursors for enhanced oxygen reduction reaction in neutral media microbial fuel cells, Energy Environ. Sci. 9 (7) (2016) 2346–2353, https://doi.org/10.1039/C6EE01145D.
[45] W. He, W. Yang, Y. Tian, X. Zhu, J. Liu, Y. Feng, B.E. Logan, Pressurized air cathodes for enhanced stability and power generation by microbial fuel cells, J. Power Sources. 332 (2016) 447–453, https://doi.org/10.1016/j.jpowsour.2016.09.112.
[46] C. Santoro, A. Stadlhofer, V. Hacker, G. Squadrito, U. Schröder, B. Li, Activated carbon nanofibers (ACNF) as cathode for single chamber microbial fuel cells (SCMFCs), J. Power Sources. 243 (2013) 499–507, https://doi.org/10.1016/j.jpowsour.2013.06.061.
[47] C.I. Torres, H.-S. Lee, B.E. Rittmann, Carbonate species as OH- carriers for decreasing the pH gradient between cathode and anode in biological fuel cells, Environ. Sci. Technol. 42 (23) (2008) 8773–8777, https://doi.org/10.1021/es8019353.
[48] R. Rossi, G. Baek, P.E. Saikaly, B.E. Logan, Continuous flow microbial flow cell with an anion exchange membrane for treating low conductivity and poorly buffered wastewater, ACS Sustain. Chem. Eng. 9 (7) (2021) 2946–2954, https://doi.org/10.1021/acssuschemeng.0c0914410.1021/acssuschemeng.0c09144.s001.
[49] P. Chong, B. Erable, A. Bergel, Microbial anodes: What actually occurs inside pores? Int. J. Hydrogen Energy. 44 (9) (2019) 4484–4495, https://doi.org/10.1016/j.ijhydene.2018.09.075.
[50] B.R. Dhar, J. Sim, H. Ryu, H. Ren, J.W. Santo Domingo, J. Chae, H.S. Lee, Microbial activity influences electrical conductivity of biofilm anode, Water Res. 127 (2017) 230–238, https://doi.org/10.1016/j.watres.2017.10.028.
[51] X. Wang, D. Li, X. Mao, E.H. Yu, K. Scott, E. Zhang, D. Wang, Anion exchange polymer coated graphite granule electrodes for improving the performance of anodes in unbuffered microbial fuel cells, J. Power Sources. 330 (2016) 211–218, https://doi.org/10.1016/j.jpowsour.2016.09.019.
[52] L. Beuth, C.P. Pfeiffer, U. Schröder, Copper-bottomed: electrochemically active bacteria exploit conductive sulphide networks for enhanced electrogeneity, Energy Environ. Sci. 13 (9) (2020) 3102–3109, https://doi.org/10.1039/D0EE01281E.